

**EXPERIMENTAL CRATERING IN QUARTZITE, TUFF AND SANDSTONE: EFFECTS OF TARGET PROPERTIES AND PROJECTILE SIZE ON CRATER DIMENSIONS.** M. H. Poelchau<sup>1</sup>, T. Hoerth<sup>2</sup>, Michael Rudolf<sup>1</sup>, A. Deutsch<sup>3</sup>, K. Thoma<sup>2</sup>, F. Schäfer<sup>2</sup>, T. Kenkmann<sup>1</sup>. <sup>1</sup>Institut für Geo- und Umweltnaturwissenschaften, Universität Freiburg, D79104 Freiburg, Germany, <sup>2</sup>Fraunhofer Ernst-Mach-Institut (EMI), Freiburg, <sup>3</sup>Institut f. Planetologie, WWU Münster, (michael.poelchau@geologie.uni-freiburg.de).

**Introduction:** With the increase in resolution of cameras onboard of current remote sensing missions, small impact craters on planetary surfaces can be observed at increasingly high detail on the meter scale and even below. At this size, target material properties play a dominant role in the formation and final shape of these craters. Therefore, the study of the effects of parameters like compressive and tensile strength or porosity can in cratering experiments is expected to give insights into the cratering process in the strength regime. The MEMIN research unit has been actively pursuing these goals. Following experimental campaigns that focused on dry and water-saturated sandstone targets [1,2], we have expanded the range of target materials to quartzite and tuff.

**Cratering Experiments:** Seven impact experiments were performed at the two-stage light-gas gun facilities of the Ernst-Mach Institute [3] on quartzite and tuff targets. Spherical D290-1 steel projectiles with diameters of 2.5 and 12 mm were accelerated to ~5 km/s. Targets were 20 cm edge length cubes and 80x80x50 cm blocks. As with previous experiments on sandstone, the impacts were recorded with high-speed cameras; ultrasound sensors were attached to the targets and ejecta particle catchers were set up opposite of the target surface (see [2] for an overview). The crater dimensions were determined with a 3D laser scanner.

Quartzite and tuff as target materials were chosen to cover a wider range of porosities in comparison to the previously used *Seeberger* sandstone (23% porosity). The quartzite (*Taunusquarzit*) has <1% porosity. Its uniaxial compressive strength (UCS) is currently being measured and is estimated at 300 MPa. The tuff (*Weiberner Tuff*) has 40% porosity and a UCS of 23.1 MPa. In one of the experiments, a 20 cm tuff target was saturated with water to ~50%.

**Results:** Crater profiles generated from the 3D scans show that quartzite targets have flatter and shallower morphologies compared to tuff targets, which show a deep penetration channel along with a narrower spall zone at the surface (Fig. 1). Small fragments of the projectile were also observed that were embedded in the crater subsurface of the tuff. The water-saturated tuff has a similar depth as the dry tuffs but is wider.

Depth-diameter ratios ( $d/D$ ) are much higher for dry tuffs (0.5) than for quartzites (0.17). Craters in

*Seeberger* sandstone have  $d/D$  values in between the two (0.2). The increase in  $d/D$  is thus correlated with decreasing target density and the corresponding increase in target porosity. The water-saturated tuff shows a decrease in  $d/D$  to 0.31 and thus shows a similar behavior to water-saturated sandstones, indicating that pore-space saturation counteracts porosity effects.

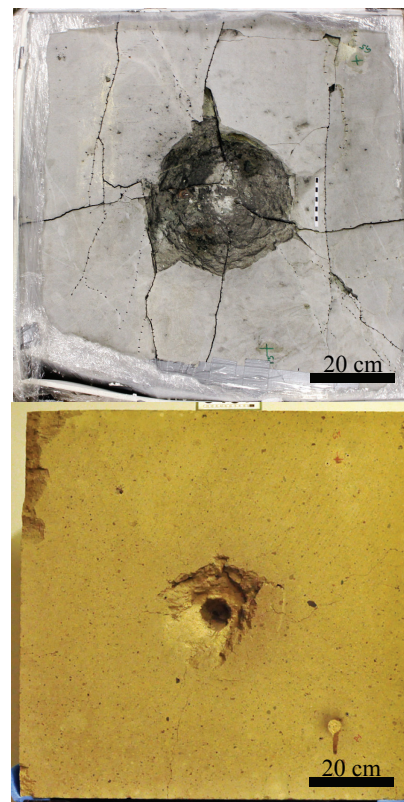


**Fig. 1:** Experimental impact craters formed in a quartzite target (top) and tuff target (bottom). Craters were formed by a 12 mm steel projectile at ~5 km/s. Targets are 80x80 cm.

Crater Volumes of experiments performed under the same conditions in dry tuff, quartzite and dry sandstone are all similar, despite the large range of target strengths. In the strength regime, crater volumes are affected by the target's strength and porosity. An increase in either value reduces crater size. Interestingly, a rock's UCS is usually reduced for increasing porosity values, following a power law, e.g. [4]. Saturating pore space with water leads to an increase in crater volume in both tuff and sandstone by reducing the

dampening effects of porosity on the shock wave, while keeping the target’s UCS roughly constant.

**Strength Scaling:** As both porosity and strength are important factors for crater size,  $\pi$ -group scaling can be used to factor out the effects of target strength. In Fig. 2a, the cratering efficiency  $\pi_V = V \rho_t / m$ , where  $V$  is the crater volume,  $\rho_t$  is the target density, and  $m$  is the projectile mass, is plotted against the strength-scaled size parameter  $\pi_3 = Y / \rho_t v_i^2$ , where  $Y$  is the uniaxial compressive strength and  $v_i$  is the impact velocity.

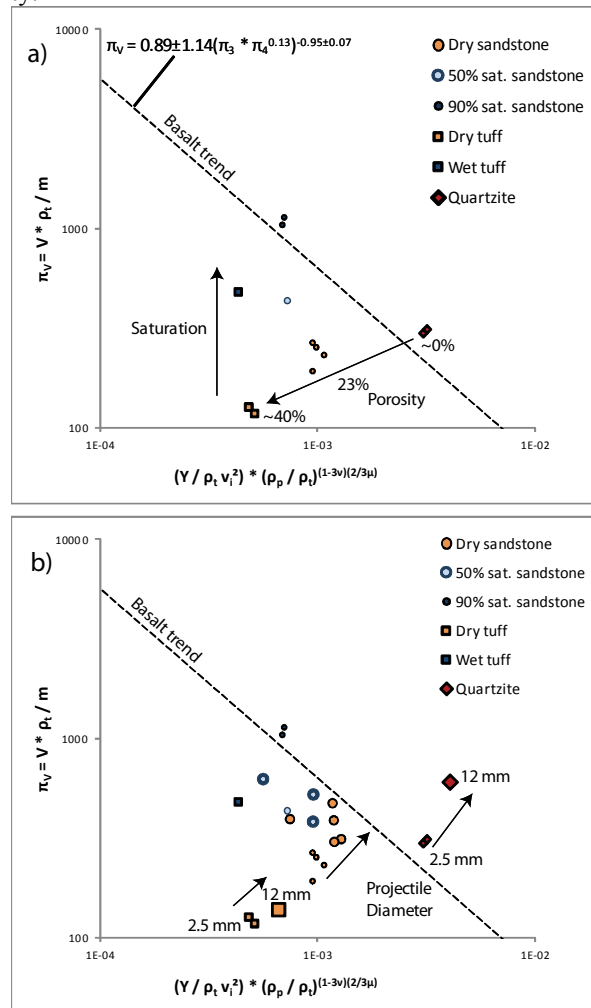


**Fig. 2:** Strength scaling of experimental crater volumes. a) Experiments in a range of target materials using 2.5 mm D290-1 steel projectiles at 5 km/s. Craters in non-porous quartzite targets lie near the trend for basalt craters [5], while craters in higher-porosity targets lie further away from the basalt trend and have lower cratering efficiencies. Water-saturation counteracts porosity effects while keeping strength values (and  $\pi_3$ -values) roughly constant. In b) experiments with 10-12 mm projectiles at ~5 km/s are added (large symbols), showing the effect of larger projectile diameters on spallation.

The trend of impact craters in basalt targets [5] is shown in Fig. 2a, and non-porous quartzites lie close to this trend, while lower-strength sandstone and tuff targets with higher porosities lie further to the left of this curve and thus have much lower cratering efficiencies than expected for their (non-porous)  $\pi_3$  values. As discussed in [2], increasing pore-space saturation effectively reduces porosity effects on crater volume and cratering efficiency, and these values lie closer to the non-porous basalt trend.

An effect that was not anticipated is the increase in cratering efficiency related to the size of the projectile (Fig. 2b). One of the advantages of the EMI’s “XL” light gas gun [3] is its capability to accelerate large projectiles to hypervelocity, thus experiments are available with a range of projectile diameters over half an order of magnitude (2.5-12 mm). Larger projectiles generate a longer pressure pulse upon impact. These longer pressure pulses increase the number of tensile fractures formed and also reduce the pressure threshold at which tensile fractures form [6,7]. This leads to larger volumes of spalled material in the craters relative to the transient crater, as shown for sandstone targets [2] and as now visible for quartzites and, to a lesser degree, tuff. The effect appears to be stronger for higher-strength materials, and is presumably due to the correlation between spall thickness and the target’s tensile strength, which are proposed to be directly proportional [8].

**Outlook:** Our results stress the importance of discerning spallation effects in cratering from the formation of transient craters, if crater volumes are to be adequately compared and scaled up to planetary dimensions. We intend to determine transient craters in the quartzite and tuff targets, using the method applied to sandstone craters in [9], and thus compare in further detail how material parameters effect the formation of experimental impact craters.

**Acknowledgements:** The MEMIN program is supported by the DFG (Research Unit FOR-887; KE-732/16-1, TH 805/4-1).

**References:** [1] Kenkmann T. et al. (2011) *M&PS*, 46, 890–902. [2] Poelchau et al. (2013) *M&PS*, 48, in press. [3] Lexow et al. (2013) *M&PS*, 48, in press. [4] Palchik, V. 2006. *Int. Jour. Rock Mech. Mining Sci.* 43, 1153–1162. [5] Moore H. J. et al. (1963) *Proc. Hyperv. Impact Sym. 6th*, 5, 367-400. [6] Ahrens T. J. and Rubin A. M. (1993) *JGR* 98, 1185–1203. [7] Meyers M. A. (1994) *Dynamic behavior of materials*. New York: Wiley, 668 p. [8] Melosh H. J. (1984) *Icarus* 59, 234–260. [9] Dufresne et al. (2013) *M&PS*, 48, in press.